Optical Fiber Technology 20 (2014) 261–267

Contents lists available at ScienceDirect

Optical Fiber Technology

www.elsevier.com/locate/yofte

Full-duplex fiber-wireless link with 40 Gbit/s 16-QAM signals for alternative wired and wireless accesses based on homodyne/heterodyne coherent detection

Ruijiao Zhang, Jianxin Ma *, Zhao Wang, Junjie Zhang, Yanjie Li, Guoli Zheng, Wen Liu, Jianguo Yu, Qi Zhang, Qin Wang, Renhao Liu

School of Electronic Engineering, Beijing University of Posts and Telecommunications, 100876 Beijing, China

ARTICLE INFO

Article history:
Received 4 November 2013
Revised 3 January 2014
Available online 27 March 2014

Keywords:
Fiber-wireless access
Full-duplex link
QAM (quadrature amplitude modulation)
Tunable laser
Homodyne/heterodyne coherent detection
Hybrid optical network unit (HONU)

ABSTRACT

A novel full-duplex fiber-wireless link with 40 Gbit/s 16-ary quadrature amplitude modulation (QAM) signals is proposed to provide alternative wired and wireless accesses for the user terminals. In the central station (CS), the downstream signal for wired and wireless accesses is beared onto the CW laser source via an optical I/Q modulator to realize the QAM modulation. At the hybrid optical network unit (HONU), a tunable laser is used to provide coherent optical local oscillator for homo-/heterodyne beating to coherently down-convert the baseband optical signal to the baseband electrical one for wired access or to the mm-wave one for wireless access according to the requirement of the user terminals. Simultaneously, the lightwave from the tunable laser is also used as the uplink optical carrier for either wired or wireless access, and is modulated colorlessly by the baseband or mm-wave signal of the uplink alternatively. After filtering, only one tone carrying the uplink signal is transmitted back to the CS even for the wireless access. The theoretical analysis and simulation results show that our proposed full-duplex link for the alternative wired and wireless accesses maintains good performance even when the transmission link with standard single mode fiber (SSMF) is extended to 30 km.

1. Introduction

With the rapid increase in the number of clients and proliferation of emerging bandwidth-hungry applications, such as, HDTV distribution and interactive multimedia services, the access network traffic has grown exponentially. The current low-speed, narrow bandwidth access communications hardly meet the requirements of high data rate and huge bandwidth. Thus, the next generation access network aims to provide high capacity and high mobility. The optical fiber access network can provide huge bandwidth and solidly support the data and video applications, but its flexibility is limited. While the current wireless access network can provide mobility by fully addressing the constraints of the wireline, it cannot meet the future wireless communications of large capacity and diversity requirements because of its limited spectrum resource and its vulnerable to a variety of damages. Recently, the radio-over-fiber (RoF) technology, integrating the advantages of optical communication and wireless communication, has become a potential candidate for the future broadband wireless system [1]. On the other hand, with the heterodyne coherent detection developing, the mm-wave signal for wireless access can be generated by using a local oscillator laser as the beat frequency source at the ONU by heterodyne coherent detection technique [2–4]. In order to satisfy the huge bandwidth, high data rate and flexible access requirements in the next generation access network, the hybrid fiber-wireless access network is emerging as a promising access network configuration, which can provide both wired and wireless accesses. Several advanced designs have been lately reported on the hybrid fiber-wireless access [5–8]. Millimeter-wave over fiber with independent wired and wireless signals has been reported [5]. By modulating wired and wireless data onto optical carrier and sub-carriers, respectively, and then separating them at remote node (RN), it can transport 10-Gbps wired and 2.5-Gbps 60-GHz wireless signals on a single wavelength simultaneously for the same user terminal. However, if both wireless and wired signals are upgraded to 10-Gbps or beyond, the narrow-band optical filter for separating the wired signal from the wireless one will be more critical. Another scheme is proposed to solve this issue [6], in which, using polarization division multiplexed technology, the wired and wireless signals are carried by the orthogonally

* Corresponding author.
E-mail address: majianxinxy@163.com (J. Ma).

http://dx.doi.org/10.1016/j.yofte.2014.02.008
1068-5200/

polarized lightwaves from a single laser source. Unlike conventional 60-GHz millimeter-wave over fiber, it may suffer from signal degradation due to optical spectrum aliasing when operated at high bit-rate, and the polarization tracing control is required to ensure that wireless and wired signals are divided on x-polarization and y-polarization completely, which makes the system complex. Moreover, the intra-channel nonlinearity, polarization fluctuation and the mutual interference between two polarized downlink channels also degrade the signal performance. In such schemes, the system is a simple combination of the wired and wireless links, and the transmitters and receivers of the wired and wireless signals are independent, which makes insufficient use of the equipments and sources. In [7,8], a laser, whose output frequency is different from the optical carrier of the downlink signal, is used as the optical local oscillator in ONU adopting polarization-division-multiplexing quadrature-phase-shift-keying (PDM-QPSK) modulation. The high speed data signal for the wired access can be used for the wireless access by optical polarization-diversity heterodyne beating. But the uplink transmission for wired or wireless access is not considered in these schemes. To further simplify the spectral structure, and to improve the spectrum efficiency, the full-duplex link with alternative wired and wireless accesses needs to be investigated.

In this paper, we have proposed a novel full-duplex fiber-wireless link for the alternative wired and wireless accesses. In the CS, an optical I/Q modulator which consists of two parallel Mach–Zehnder modulators (MZMs) with $\pi/2$ phase shift is used to modulate the 16-QAM vector signal onto the optical carrier. After transmitted over the SSMF to HONU, the data-bearing optical signal can be demodulated in homodyne or heterodyne coherent detection pattern according to the requirement of the user terminals by tuning the wavelength of the optical local oscillator for alternative wired or wireless access. The optical local oscillator is simultaneously used as the optical carrier for the uplink. And the baseband or the 60-GHz 16-QAM mm-wave uplink signal received by the antenna from the user terminals is modulated onto the optical local oscillator via a MZM and then transmitted back to the CS. In our scheme, the full-duplex fiber-wireless link can provide wired or wireless access alternatively, and can tune the output frequency of the tunable laser at HONU to obtain the desired electrical mm-wave not only the 60-GHz mm-wave according to the requirement of the wireless user terminals. To verify the feasibility, the full-duplex link for alternative wired and wireless accesses is built up in the simulation platform, and the simulation results show that the full-duplex fiber-wireless link has good performance for both wired and wireless accesses.

The paper is organized as follows. In Section 2, the principle of the proposed full-duplex for the alternative wired and wireless accesses is described and the transmission performances of both wired and wireless accesses are analyzed theoretically. In Section 3, a concept-proof full-duplex fiber-wireless link based on the simulation platform is built and the simulation results are analyzed. At last, a conclusion is given in Section 4.

2. Principle of operation

Our proposed full-duplex fiber-wireless link is shown in Fig. 1. In the CS, the lightwave, emitted from the CW laser with the central frequency of $f_0 = \omega_0/2\pi$, can be expressed as

$$E(t) = E_0 e^{j\omega_0 t} \tag{1}$$

where E_0 is the amplitude of the lightwave electrical field, and ω_0 is its central angular frequency. Firstly, the lightwave is equally power split into two beams by an optical coupler. One beam is modulated by the QAM signal $S(t) = I(t) + jQ(t)$ via an optical I/Q modulator as shown in Fig. 1. The other beam is reserved as the optical local oscillator for the uplink signal demodulation.

According to the transmission function of the nested MZM and the operating principle of the optical I/Q modulator, the data-bearing optical signal after data modulation can be expressed as

$$\begin{aligned} E_0^1(0,t) &= \gamma_1 E(t)\left[\sin\pi\frac{V_m}{V_\pi}I(t) + j\sin\pi\frac{V_m}{V_\pi}Q(t)\right] \\ &\approx \gamma_1 m_{h1} E(t)[I(t) + jQ(t)] = \gamma_1 m_{h1} E_0[I(t) + jQ(t)]e^{j\omega_0 t} \end{aligned} \tag{2}$$

here modulation index is defined as $m_{h1} = \pi V_m/V_\pi$, γ_1 is the downlink LN-MZM insertion loss and the approximation is proper if the modulation index is much smaller than 1. The data-bearing optical signal is transmitted along the chromatic fiber with the amplitude attenuation coefficient of α and propagation constant of $\beta(\omega)$ at the angular frequency of ω. If the nonlinearity is neglected, the fiber transmission function with the length of z can be expressed in frequency domain as

$$H(\omega) = e^{-\alpha z} e^{-j\beta(\omega)z} \tag{3}$$

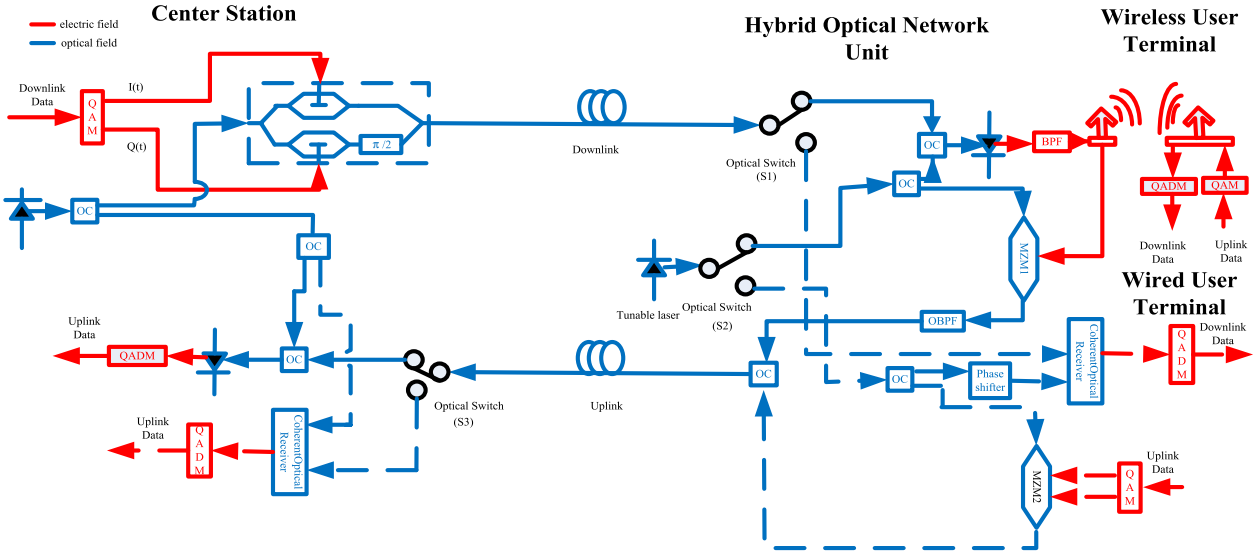

Fig. 1. The full-duplex hybrid fiber-wireless access link.

And so the data-bearing optical signal transmitted over the fiber can be expressed mathematically as

$$E_0^1(z,t) = F^{-1}\{H(\omega)F\{E_0^1(0,t)\}\} \tag{4}$$

here $F\{\ \}$ and $F^{-1}\{\ \}$ are the forward and inverse Fourier transforms, respectively. Instituting Eqs. (2) and (3) into Eq. (4), we obtain

$$\begin{aligned} E_0^1(z,t) &= F^{-1}\{H(\omega)F\{E_0^1(0,t)\}\} \\ &= F^{-1}\{e^{-\alpha z}e^{-j\beta(\omega)z}\gamma_1 E_0[-I(\omega-\omega_0)+jQ(\omega-\omega_0)]\} \\ &= \gamma_1 E_0 e^{-\alpha z}F^{-1}\{e^{-j\beta(\omega)z}[-I(\omega-\omega_0)+jQ(\omega-\omega_0)]\} \end{aligned} \tag{5}$$

Since $\beta(\omega)$ can be expanded in Taylor's serial at the angular frequency of ω_0 approximated as

$$\beta(\omega) = \beta(\omega_0) + \beta'(\omega_0)(\omega-\omega_0) + \cdots \tag{6}$$

Eq. (5) becomes

$$\begin{aligned} E_0^1(z,t) &= F^{-1}\{H(\omega)F\{E_0^1(0,t)\}\} = \gamma_1 E_0 e^{-\alpha z}F^{-1}\{e^{-j\beta(\omega)z}[-I(\omega-\omega_0) \\ &\quad +jQ(\omega-\omega_0)]\} \\ &\approx \gamma_1 E_0 e^{-\alpha z}F^{-1}\{e^{-j(\beta(\omega_0)+\beta'(\omega_0)(\omega-\omega_0))z}[-I(\omega-\omega_0) \\ &\quad +jQ(\omega-\omega_0)]\} \\ &= \gamma_1 E_0 e^{-\alpha z}e^{-j\beta(\omega_0)z}e^{j\beta'(\omega_0)\omega_0 z}F^{-1}\{e^{-j\beta'(\omega_0)\omega z}[-I(\omega-\omega_0) \\ &\quad +jQ(\omega-\omega_0)]\} = \gamma_1 E_0 e^{-\alpha z}[-I(t-\tau) \\ &\quad +jQ(t-\tau)]e^{j[\omega_0 t-\beta(\omega_0)z]} \end{aligned} \tag{7}$$

here we assume $\beta'(\omega_0)z = \tau$, which denotes the transmission delay. In our theoretical analysis, the 2nd and the higher-order derivatives of $\beta(\omega)$ are ignored since they have little impact on the signal with baud rate smaller than 10GS/s because the fiber link between the OLT and the ONU is usually no more than 100 km in the optical access network. In our scheme, the transmission distance is below 30 km and the date rate is below 10 GS/s. To confirm this assumption, the effects of 2nd and higher-order derivatives on the optical signal performance are emerged by the constellation and the EVM curves in the simulation.

After transmitted over the optical fiber, the downlink optical signal can be demodulated in different patterns according to the requirement of the access user terminals connected to the HONU. At the HONU, firstly, an optical switch (S1) is employed to switch the downlink optical signal to the different optical-electrical conversion modules where the signal can be demodulated in different patterns according to the access terminals for the wired or wireless access. The dotted line in Fig. 1 shows the wired access while the solid line shows the wireless access. Another optical switch (S2) switches the tunable laser in the same way as S1. The lightwave from the tunable laser is used as the optical local oscillator for homodyne/heterodyne as well as the optical carrier for the uplink data and its output can be expressed as $E_1(t) = E_1\exp(j\omega_1 t)$. It is noted that in our simulation system, which is an ideal working condition, at the HONU, we only tune the output wavelength of the tunable laser with the same frequency as the downlink optical signal for wired connection, or make proper frequency spacing away from the downlink optical signal for wireless connection without any DSP process. But, in the real system, the frequency tracing module based on DSP is necessary to assure the LO frequency exactly match that of the Tx laser for wired access and keep a fixed frequency away from that of the Tx laser for the wireless access, respectively. The frequency offset and phase drift from the photocurrent carrying the 16-QAM signal are abstracted and then are converted to the control signals for feedbacking the local oscillator laser, to realize the frequency tracing and phase recovery.

For the wired access, the frequency of the lightwave emitted from the tunable laser is tuned to be equal to the downlink data-bearing optical signal, namely $\omega_1 = \omega_0$. They are injected into an optical coherent receiver, which consists of an optical phase shifter, a 2-input–4-output optical 90° hybrid and two pairs of balanced photo-diodes (PDs), to demodulate the downlink optical signal based on the homodyne coherent detection. The optical phase shifter is used to introduce a relative phase shift $\Delta\varphi$ to match the phase between the downlink optical signal and the optical local oscillator, so the optical local oscillator becomes $E_1'(t) = E_1\exp[j(\omega_1 t + \Delta\varphi)]$. The outputs from 4-port optical hybrid are expressed as

$$\begin{pmatrix} E_{output1}(z,t) \\ E_{output2}(z,t) \\ E_{output3}(z,t) \\ E_{output4}(z,t) \end{pmatrix} = \frac{1}{2}\begin{pmatrix} jE_1'(t) - jE_0^1(z,t) \\ E_1'(t) + E_0^1(z,t) \\ -jE_1'(t) - E_0^1(z,t) \\ -E_1'(t) - jE_0^1(z,t) \end{pmatrix} \tag{8}$$

Two pairs of balanced detectors following the optical hybrid are used to convert the optical QAM signals to the electrical ones. Each balanced detection pair consists of two square-law PDs with the opto-electrical conversion relationship, $I(z,t) = \mu|E(z,t)|^2$, here μ is the sensitivity of PD. Considering the balanced configuration of the receiver PDs, the output photocurrents of the receiver signal can be expressed as

$$\begin{aligned} I_I(z,t) &= I_1(z,t) - I_2(z,t) = \mu[|E_{output1}(z,t)|^2 - |E_{output2}(z,t)|^2] \\ &= 4\mu\gamma_1 E_0 E_1 e^{-2\alpha z}[I(t-\tau)\cos(-\beta(\omega_0)z - \Delta\varphi) \\ &\quad + Q(t-\tau)\sin(-\beta(\omega_0)z - \Delta\varphi)] \end{aligned} \tag{9}$$

$$\begin{aligned} I_Q(z,t) &= I_3(z,t) - I_4(z,t) = \mu[|E_{output3}(z,t)|^2 - |E_{output4}(z,t)|^2] \\ &= 4\mu\gamma_1 E_0 E_1 e^{-2\alpha z}[Q(t-\tau)\cos(-\beta(\omega_0)z - \Delta\varphi) \\ &\quad - I(t-\tau)\sin(-\beta(\omega_0)z - \Delta\varphi)] \end{aligned} \tag{10}$$

here, if the optical phase shifter is adjusted to assure $\beta(\omega_0) - \Delta\varphi = 2k\pi$ ($k = \pm1, \pm2, \pm3, \ldots$), the downlink QAM optical signal is correctly demodulated at the HONU and can be expressed as

$$I_I(z,t) = 4\mu\gamma_1 E_0 E_1 e^{-2\alpha z} I(t-\tau) \tag{11}$$

$$I_Q(z,t) = 4\mu\gamma_1 E_0 E_1 e^{-2\alpha z} Q(t-\tau) \tag{12}$$

For the wired access uplink, the uplink vector signal $S_{up}(t) = I_{up}(t) + jQ_{up}(t)$ is modulated onto the reserved optical carrier provided by the tunable laser in the same way as that of the downlink transmitter in the CS. The modulated uplink optical signal can be expressed as

$$\begin{aligned} E_{up-wired}(t) &= \gamma_2 E_1(t)\left[\sin\pi\frac{V_{up}}{V_\pi}I_{up}(t) + \sin\pi\frac{V_{up}}{V_\pi}Q_{up}(t)\right] \\ &\approx \gamma_2 m_{h2} E_1(t)[I_{up}(t) + jQ_{up}(t)] \\ &= \gamma_2 m_{h2} E_1[I_{up}(t) + jQ_{up}(t)]e^{j\omega_0 t} \end{aligned} \tag{13}$$

here $m_{h2} = \pi V_{up}/V_\pi$ is the uplink modulation index, γ_2 is the uplink LN-MZM insertion loss and the approximation is also proper if m_{h2} is much smaller than 1. After transmitted over the uplink, the uplink optical signal becomes

$$E_{up\text{-}wired}(z',t) = \gamma_2 E_1 e^{-\alpha z}[I_{up}(t-\tau') + jQ_{up}(t-\tau')]e^{j(\omega_0 t - \beta(\omega_0)z)} \tag{14}$$

here the transmission delay of the uplink is $\beta'(\omega_0)z' = \tau'$. In the CS, the reserved optical local oscillator at ω_0 is used to coherently demodulate the uplink optical signal into electrical one via an optical coherent receiver. At this condition, the full-duplex link has a symmetrical structure.

For the wireless access, the tunable laser at the HONU is tuned to keep a frequency spacing $\Delta\omega = |\omega_1 - \omega_0|$, which is equal to the frequency of the desired electrical mm-wave, between the optical local oscillator emitted from it and the downlink optical signal. Then the optical local oscillator and downlink optical signal are

injected into the high-speed square law PD to convert to the desired electrical mm-wave based on heterodyne beating detection, and the photocurrent can be expressed as

$$\begin{aligned} I_{down\text{-}wireless}(t) &= \mu'|E(z,t)+E_1(t)|^2 = \mu'|\gamma_1 E_0 e^{-\alpha z}[I(t-\tau) \\ &\quad + jQ(t-\tau)]e^{j(\omega_0 t-\beta(\omega_0)z)} + E_1 e^{j\omega_1 t}|^2 \\ &= \mu'\Big\{E_1^2 + \gamma_1^2 E_0^2 e^{-2\alpha z}(I^2(t-\tau)+Q^2(t-\tau)) \\ &\quad - 2\gamma_1 E_1 E_0 e^{-\alpha z}[I(t-\tau)\cos((\omega_0-\omega_1)t-\beta(\omega_0)z) \\ &\quad + Q(t-\tau)\sin((\omega_0-\omega_1)t-\beta(\omega_0)z)]\Big\} \end{aligned} \tag{15}$$

here μ' is the sensitivity of the PD for the wireless access at the HONU. Then, the mm-wave signal at frequency of $|\omega_1-\omega_0|$ in the photocurrent is abstracted out and directly radiated to the mobile user terminals via the antenna after amplification. The mobile user terminal receives the mm-wave signal and coherently demodulates the downlink signal to the baseband one.

For the wireless uplink, the optical carrier from the tunable laser is modulated by the uplink QAM electrical mm-wave signal from the antenna via a MZM, and generates sidebands around the optical carrier. One optical sideband at $(\omega_1+\omega_{RF})$ bearing the uplink data signal is abstracted out by an optical band-pass filter and transmitted back to the CS through the uplink. In the CS, the reserved optical local oscillator at ω_0 is used to coherently demodulate the uplink optical signal into the baseband electrical one if $\omega_1+\omega_{RF}=\omega_0$. Otherwise, the uplink optical signal is converted to the IF electrical signal with the frequency at $|\omega_0-\omega_1-\omega_{RF}|$ via a PD by the heterodyne beating and then coherently demodulated to the baseband signal.

The proposed scheme can realize the full-duplex fiber-wired and wireless accesses alternatively with the baseband signal transmitted in optical domain. Using a tunable laser at the HONU to provide the optical local oscillator, the downlink optical signal can be demodulated in homodyne or heterodyne pattern for the wired or wireless access, respectively. The uplink optical carrier can also be obtained from the tunable laser. In our scheme, whether wired or wireless access is provided by the full-duplex optical link, the structure of CS and the downlink optical spectrum are identical, which simplifies the CS. The user terminals can neatly choose the access pattern. Moreover, the frequency of the desired electrical mm-wave signal can be tuned freely by varying the output frequency of the tunable laser.

3. Simulation setup and results

In order to verify our proposed scheme of the full-duplex fiber-wireless link for the wired and wireless alternative accesses, a concept-proof optical link based on the OptiSystem platform is built. In the CS, the continuous lightwave with the frequency of 193.1 THz and the line-width of 100 kHz is emitted from the LD and is power split into two beams (B1 and B2) by an optical coupler, as shown in Fig. 2(a). One beam (B1) is modulated by the 16-ary QAM data signal, which is mapped from the 40 Gbit/s PRBS with the word length of 2^9-1, via a nested I/Q modulator with the half-wave voltage of 4 V. The other (B2) is reserved as the optical local oscillator to demodulate the uplink optical signal. The downlink optical signal, shown by the optical spectrum in Fig. 2(b), is transmitted to HONU over the SSMF with chromatic dispersion D = 16.75 ps/km/nm, power attenuation coefficient of 0.2 dB/km. At the HONU, the lightwave from a tunable laser is power split into two beams (B3 and B4). One beam (B3) is used as the optical local oscillator to coherently demodulate the downlink optical signal. The other (B4) is used as optical carrier for the uplink data.

At the HONU, the downlink optical signal can be demodulated in different patterns according to the requirement of the user terminals. For the wired access, the full-duplex optical link is switched to the wired port, as shown in Fig. 2. The lightwave (B3), which is emitted from the tunable laser and used as the optical local oscillator, is tuned to have the same frequency as the data-bearing downlink optical signal at 193.1THz. After matching their relative phase by an optical phase shifter, the downlink optical signal along with the optical local oscillator is injected into an optical coherent receiver and coherently demodulated to the electrical baseband one with I- and Q- branches.

For the wired access uplink, the reserved beam (B4) at 193.1THz is baseband modulated by the 16-QAM uplink signal and transmitted back to the CS over the uplink, whose optical spectrum is shown in Fig. 2(c). In the CS, the reserved optical local oscillator (B2) at 193.1 THz is used to coherently demodulate the uplink optical signal to the electrical baseband one by an optical coherent receiver.

The EVM and Bit Error Rate (BER) are commonly used to evaluate the performance of the received signal. The EVM can be obtained from the optimized constellation diagrams, while the BER describes the probability of error in terms of number of erroneous bits per bit transmitted. Considering M-ary modulation, the relationship between the EVM and BER for the 16-QAM vector signal can be expressed by [9]

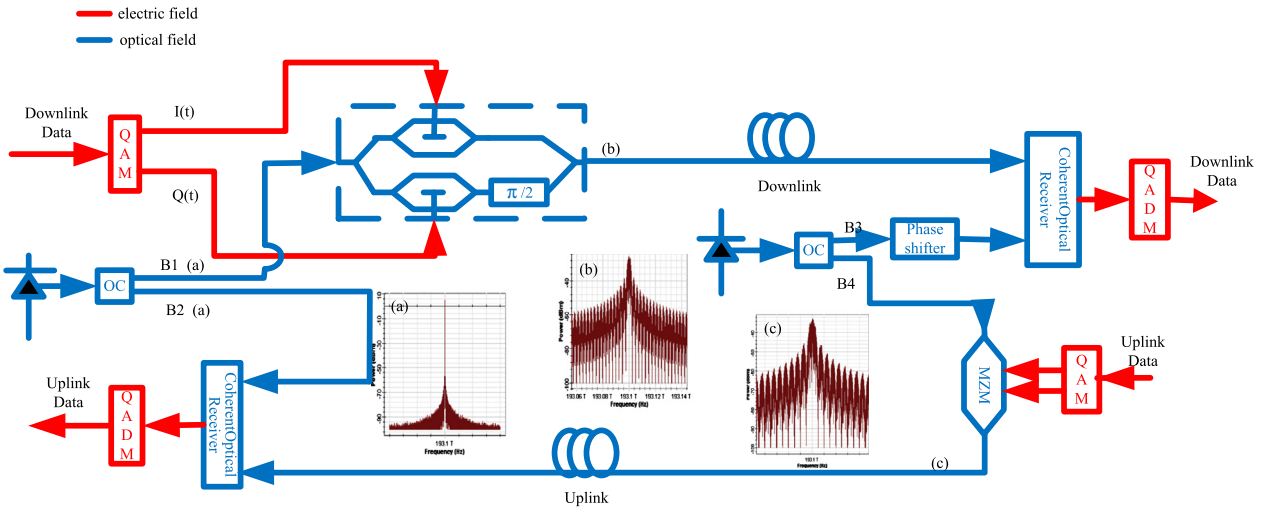

Fig. 2. The full-duplex link with alternative wired and wireless access for wired access.

$$BER = \frac{3}{4}Q\left[\sqrt{\frac{1}{5EVM^2}}\right] \tag{16}$$

where $Q(\cdot)$ is the Gaussian co-error function and is given by $Q(x) = \int_x^\infty \frac{1}{\sqrt{2\pi}} e^{\frac{-y^2}{2}} dy$. Fig. 3 shows the curve of BER versus EVM for 16-QAM vector signal.

From Fig. 3 we can see that for the 16-QAM vector signal the BER is proportional to EVM. When the EVM is 16%, the BER is about 1.9×10^{-3} which is below the FEC limit of BER of 2.3×10^{-3} [10]. But when the EVM is 18%, the BER is about 4.9×10^{-3} which exceeds the FEC limit. So, we must control the EVM under the 16% for the 16-QAM vector signal

In our scheme, in order to check the signal performance of the down- and up-link for wired access, we only use the EVM curves and the corresponding constellation at a certain received power of the down- and up-link 16-QAM signals for wired access without forward error correction (FEC) to evaluate the performance of the received 16-QAM signal, as illustrated in Fig. 4. It shows that the EVMs of the down- and up-link increase with the reduction of the received power and increase of the fiber length. When the received power is larger than −20 dBm, the EVM curves of down- and up-link appear floor, but the EVM increases rapidly when the received power is less than −20 dBm. At the B-T-B case, the EVMs

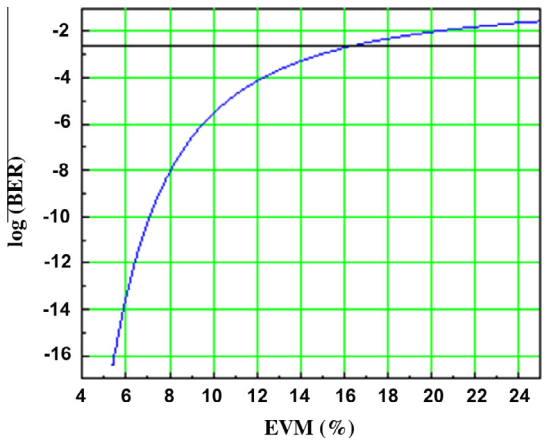

Fig. 3. The conversion relationship between EVM and BER for 16-QAM vector signal.

of the down- and up-link signals we calculated are about 7% when the receiver power is −17 dBm, while the EVM increases to 15.4% after 30 km fiber transmission, which is still below the FEC limit of BER of 2.3×10^{-3}. The clear constellation diagrams of the insets in Fig. 4 show that the constellation points get a certainly dispersive as the fiber length increases, but they do not overlap with each other and can be distinguished clearly. Noting that in both the experiment and real system, DSP is necessary for coherent detection. In our scheme, the simulation condition is ideal, so we have not use the DSP. But in the real system, DSP is necessary for processing the frequency tracing and clock recovery and equalization of the impairment from the fiber dispersion. After the frequency tracing and clock recovery by DSP, the phase noise will be canceled, and the constellation expansion along the tangential direction will disappear as shown in Fig. 4 and the following Fig. 6 for the wireless access. If a DSP is used here to compensate the dispersion, the phase noise due to the dispersion can be reduced greatly, and the transmission length will be extended greatly.

For the wireless access, the full-duplex optical link is switched as Fig. 5. The downlink is the same as that of the wired access scheme above. But at the HONU, the tunable laser is tuned to 193.04THz to assure a 60-GHz frequency spacing from the downlink data-bearing optical signal, namely, f_{down} = (193.1–193.04) THz = 60 GHz, as shown in Fig. 5(a). Then it is coupled with the downlink optical signal together, and the spectra are shown in Fig. 5(b). Then they are injected into the high-speed square law PD for heterodyne beating to generate the 60-GHz mm-wave, as shown by the RF spectrum in Fig. 5(c).

For the wireless access uplink, the reserved beam (B4) from the tunable laser at 193.04 THz at the HOUN is modulated by the 60-GHz 16-QAM uplink mm-wave signal in SSB pattern, as shown in Fig. 5(d). The optical sideband at 193.1 THz carrying the uplink data is filtered out by an optical filter and transmitted back to the CS as shown by the spectrum in Fig. 5(e). By this means, the optical millimeter-wave signal is down-converted to the baseband in optical domain which occupies a much narrow bandwidth. In the CS, the reserved optical local oscillator (B2) at 193.1THz is used to coherently demodulate uplink optical signal to the electrical baseband one with I- and Q- branches.

Fig. 6 presents the measured EVM curves and the corresponding constellation diagrams of the down- and up-link 16-QAM signals for wireless access. It can be seen that as the wired access, the EVM floor appears when the received optical power is larger than −20 dBm. When the fiber length reaches 30 km and the received

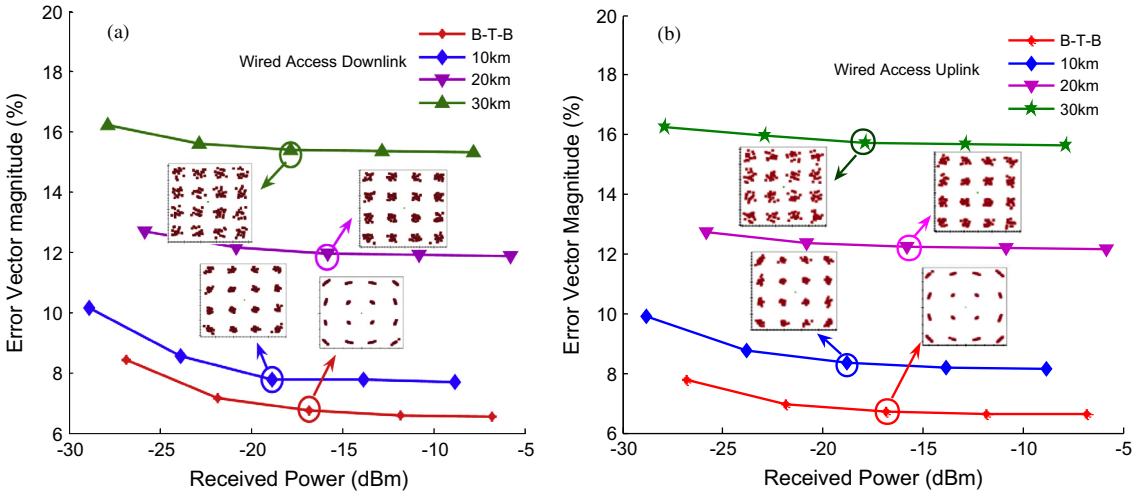

Fig. 4. The EVM curves of (a) down- and (b) up-link 16-QAM signals for wired access.

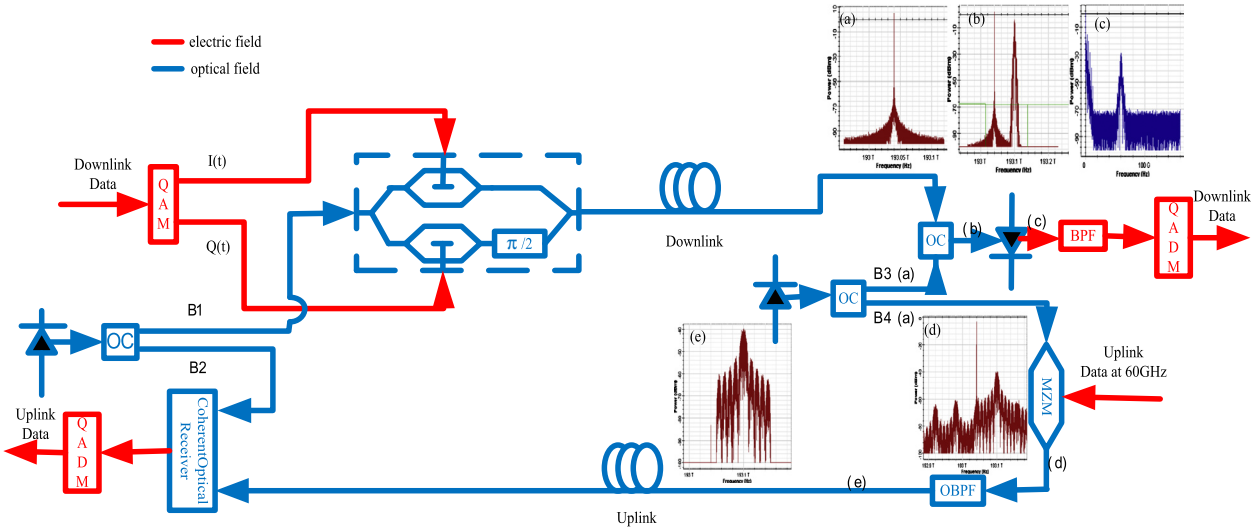

Fig. 5. The wired part of the full-duplex link with alternative wired and wireless access for wireless access.

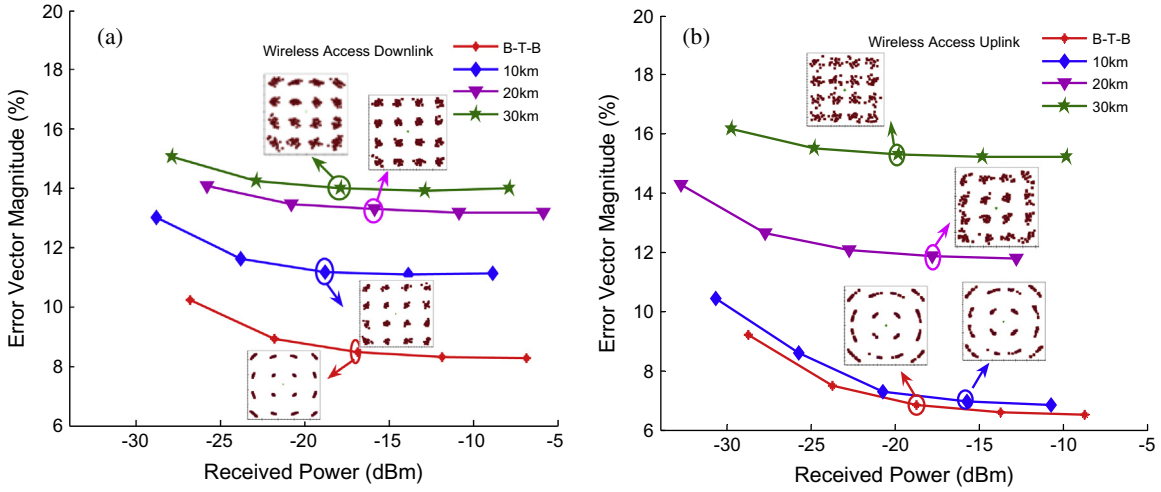

Fig. 6. The EVM curves of (a) down- and (b) up-link 16-QAM signals for wireless access.

power is about −17 dBm, the EVMs of the demodulated down- and up-link signal are about 14% and 15.2%, respectively, which can guarantee the BER below the FEC limit. Comparing the EVMs of the down-link with that of the up-link, it can be seen that the transmission performance of uplink is better than the downlink when the fiber length is less than 10 km, but the downlink is better than the uplink when the fiber length is larger than 20 km. This is because when the transmission distance is short, the fiber loss is the main factor to effect the signal performance and the fiber dispersion and nonlinearity have a little effects on the optical signal. Moreover, the optical coherent detection with improving receiver sensitivity is used to receive the uplink signal in the CS. But, with the increase of the transmission distance, the fiber dispersion and nonlinearity have a greater impact on the optical signal than the fiber loss, so the downlink outperforms the uplink. From Fig. 6, it can be also seen that the EVM floors for wireless at about 8% at B-T-B case which is larger than the wired access case, which indicates that the performance of the signal from the wired access is better than from the wireless access when the received power larger than −20 dBm. The constellation diagrams in the insets of Fig. 6 show that although the constellation points of the down- and up-link signal get an obvious dispersion as the fiber length increases which is attribute to the chromatic dispersion and nonlinear effects of the optical link, they still maintain reasonable distances from their ideal position points even if the transmission distance is extended to 30 km. This provides a good insight into the performance of the full-duplex link for the wireless access.

4. Conclusion

In this paper, we propose a novel full-duplex fiber-wireless link based on homodyne/heterodyne coherent detection for wired and wireless alternative accesses. At the HONU, using a tunable laser to provide the optical local oscillator, we can neatly tune the output frequency of the tunable laser to realize the wired or wireless access based on the homodyne or heterodyne detection and for the wireless access, we can easily tune the output frequency of the tunable laser to obtain the desired electrical millimeter-wave not only the 60-GHz one. The uplink optical carrier also is provided by the tunable laser that can simplify the structure of the HONU. Moreover, whether the wired or wireless access pattern is chosen at the HONU, the optical spectrum of the downlink optical signal is same, which reduces the complexity of the CS and simplifies the structure of the spectrum. The simulation results demonstrate

the feasibility of our proposed full-duplex link. Our proposed full-duplex fiber-wireless link is expected to be implemented in the future wired and wireless integrated network providing the wired and wireless alternative accesses for the users.

Acknowledgments

This work was supported in part by the Program for New Century Excellent Talents in University with No. NECT-11-0595, the Specialized Research Fund for the Doctoral Program of Higher Education (Grant No.: 20100005120014), and the Fundamental Research Funds for the Central Universities of China (Grant Nos.: 2013RC0209, 2013RC0201), and the National Natural Science Foundation of China (Grant Nos.: 61377079, 61201151).

References

[1] Z. Jia, J. Yu, G. Ellinas, G.K. Chang, Key enabling technologies for optical-wireless networks: optical millimeter-wave generation, wavelength reuse, and architecture, J. Lightw. Technol. 25 (11) (Nov. 2007) 3452–3471.
[2] J. Zhang, Z. Dong, J. Yu, N. Chi, L. Tao, X. Li, Y. Shao, Simplified coherent receiver with heterodyne detection of eight-channel 50 Gb/s PDM-QPSK WDM signal after 1040 km SMF-28 transmission, Opt. Lett. 37 (19) (2012) 4050–4052.
[3] X. Li, Z. Dong, J. Yu, J. Yu, N. Chi, Heterodyne coherent detection of WDM PDM-QPSK signals with spectral efficiency of 4 b/s/Hz, Opt. Express 21 (2013) 8808–8814.
[4] J. Yu, X. Li, N. Chi, Faster than fiber: over 100-Gb/s signal delivery in fiber wireless integration system, Opt. Express 21 (19) (2013) 22885–22904.
[5] M.F. Huang, A. Chowdhury, Y.T. Hsueh, J. Yu, G.K. Chang, Integration of RoF with WDM-PON for lightwave centralized access network, in: The 16th Opto-Electronices and Communication Conference, OECC 2011, July. 2011, pp. 387–388.
[6] Z. Jia, J. Yu, A. Chowdhury, G. Ellinas, G.K. Chang, Simultaneous generation of independent wired and wireless services using a single modulator in millimeter-wave-band radio-over-fiber systems, IEEE Photon. Technol. Lett. 19 (20) (2007) 1691–1693.
[7] H.C. Chien, A. Chowdhury, Y.T. Hsueh, Z. Jia, S.H. Fan, et al., A novel 60-GHz millimeter-wave over fiber with independent 10-Gbps wired and wireless services on a single wavelength Using PolMUX and wavelength-reuse techniques, in: OFC 2009, March 2009, pp. 1–3.
[8] X. Li, J. Yu, Z. Dong, Z. Cao, et al., Seamless integration of 57.2-Gb/s signal wireline transmission and 100-GHz wireless delivery, Opt. Express 20 (22) (2012) 24364–24369.
[9] R.A. Shafik, S. Rahman, R. Islam, On the extended relationships among EVM, BER and SNR as performance matrics, in: ICECE 2006, December 2006, pp. 408–411.
[10] D. Hillerkuss, R. Schmogrow, T. Schellinger, M. Jordan, et al., 26 Tbit/s line-rate super-channel transmission utilizing all-optical fast Fourier transform processing, Nat. Photon. 5 (6) (Jun. 2011) 364–371.